

## *Fundamental Characteristics of a Cylindrical Linear Pulse Motor for the Artificial Heart*

By

Hajime YAMADA,\* Michihiro YAMAMOTO,\*\* Kiwamu MURATA,\*\*\*  
Shintaro FUKUNAGA,\*\*\*\* Yukio YAMAMOTO,\*\*\*\*\*  
and Naotake NISHIZAWA\*\*\*\*\*

(Received May 31, 1984)

### **Synopsis**

A new actuator using a cylindrical linear pulse motor for the artificial heart is proposed with descriptions of the principle of operation, theoretical expression of thrust, and experimental results. The actuator has a simple configuration and its size is much smaller than the ordinary external backup facility using a pneumatic power. The actuator consists chiefly of a linear pulse motor and two rooms of sacs for the right and left ventricles. Some problems have been found to be solved before the actuator can be applied to the actual artificial heart.

### **1. Introduction**

Aiming at finally devising an implantable energy convertor for the artificial heart, the present research has attained an intermediate step to make available a new actuator by making use of a cylindrical linear pulse motor.

The new actuator for the artificial heart, Model AHA-H16, including the driver, pulse generator, and interface, weighs 5.4 kgf, the weight of the actuator itself being 1.7 kgf. Only the actuator is to be implanted in the body. In contrast, the latest type of similar American implantable device, developed in the University of Utah, requires an external backup facility weighing as much as nearly 170 kgf and two thick tubes in the chest.<sup>1)</sup>

The new actuator consists chiefly of a cylindrical linear pulse motor with rare-earth magnets, two sacs for the right and left ventricles, and connecting devices to the artificial heart.

---

\* Professor, Department of Electrical Engineering.  
\*\* Researcher, Kogyosha Co., Ltd.  
\*\*\* Graduate student, Shinshu University.  
\*\*\*\* Assistant, Hiroshima University School of Medicine.  
\*\*\*\*\* Professor, Nagano Technical College.  
\*\*\*\*\* Director of Technical Management, Orion Machinery Co., Ltd.

This paper deals with the principle of operation, theoretical expression of thrust, and experimental results for the actuator using a linear pulse motor for the artificial heart.

## 2. Principle of operation

The constitution of an ordinary air-pressure generating unit for the artificial heart is shown in Fig. 1. In general, the ordinary unit consists of a pair of air-pressure generators, pistons, gears, stepping motors, and their drivers; it requires a lot of mechanical elements and accordingly delicate adjustments for synchronous movement. The actuator developed by the present authors can replace the part indicated by the dotted line in Fig. 1.

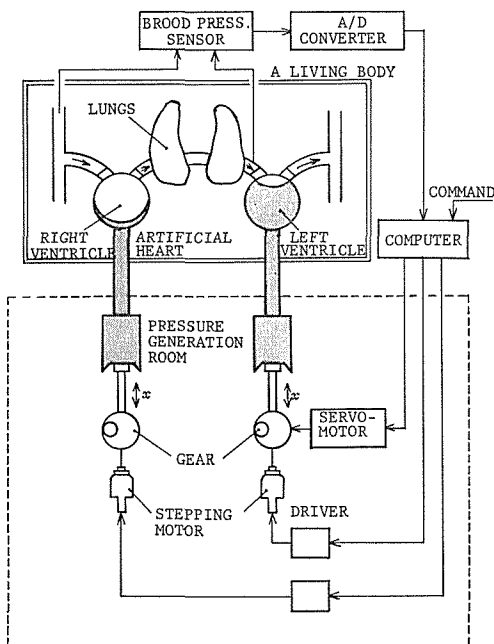


Fig.1 Constitution of an ordinary air-pressure generating unit for the artificial heart.

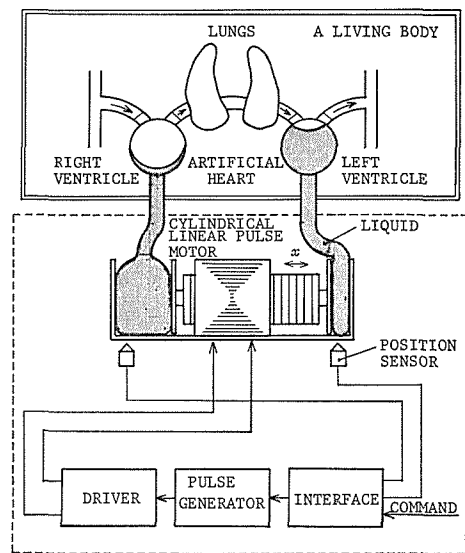


Fig.2 Constitution of the actuator using a cylindrical linear pulse motor, CLPM, for the artificial heart.

Figure 2 shows the constitution of the new actuator using a linear pulse motor for the artificial heart. The actuator consists of a cylindrical linear pulse motor, a driver, a pulse generator, and an interface.

Since the cylindrical linear pulse motor, CLPM, is designed for professional use by our group, it is provided with controls for varying frequency and thrust

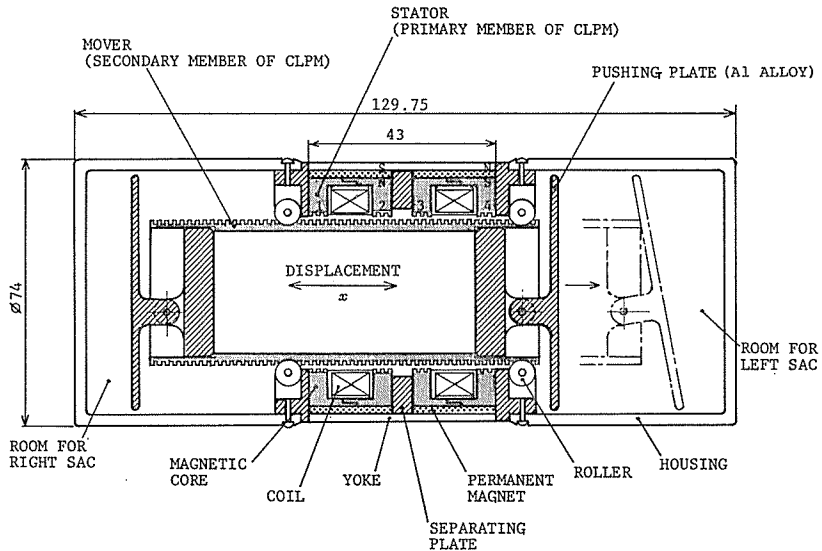


Fig. 3 Configuration of a new actuator using CLPM. (Digits 1, 2, 3, and 4 indicate the pole number).

intensity according to pulse signals from the command. The displacement,  $x$ , or stroke of CLPM can be controlled by two position sensors or an internal counter, signals from these sensors being sent to a system for feedback control.<sup>2)</sup>

The configuration of the new actuator is shown in Fig. 3. The actuator consists mainly of a stator and a mover. The stator and mover are called the pri-

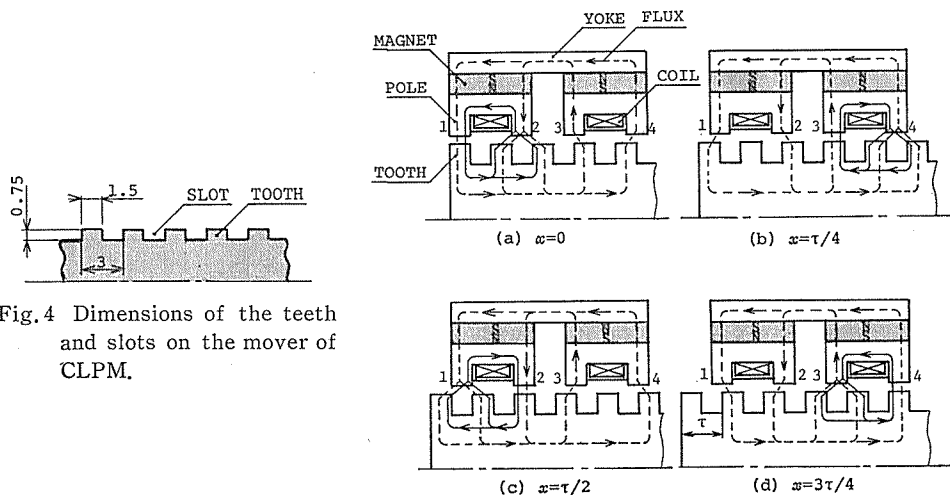


Fig. 4 Dimensions of the teeth and slots on the mover of CLPM.

Fig. 5 Principle of operation of a CLPM. ( $x$ : displacement,  $\tau$ : pitch=3.0mm.)

mary and secondary members of CLPM, respectively. The stator has two coils with permanent magnets, and the mover has a moving hollow cylindrical rod with many teeth and slots on its spherical surface.

Figure 4 shows the dimensions and shapes of the teeth and slots of the mover. The width of the tooth is 1.5 mm, equal to the width of the slot. The depth of the slot is 0.75 mm, equal to half the width of the slot. The pitch,  $\tau$ , of mover is 3.0 mm.

The principle of operation of the CLPM for one-phase excitation is shown in Fig. 5. In the figure, the solid line represents the flow of magnetic flux induced by the exciting current and the broken line represents the flow of magnetic flux produced by the permanent magnet. When the poles 1, 3, 2, and 4 are excited sequentially, the mover of CLPM is caused to move by one step,  $\tau/4$ , to the left.

### 3. Theoretical expression of the thrust of CLPM

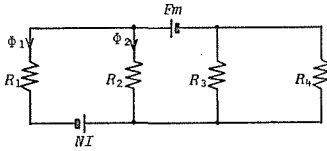


Fig. 6 Magnetic equivalent circuit of CLPM.

The magnetic equivalent circuit is constructed in Fig. 6. Symbols  $NI$  and  $F_m$  indicate the magnetomotive forces by the exciting current and the permanent magnet, respectively.  $R$  is the reluctance of air gap, its subscript indicating the pole number.

In this section, we adopt the assumption there is a linear relation between the exciting current and the magnetic flux without hysteresis. The magnetic fluxes of pole 1,  $\Phi_1$ , and pole 2,  $\Phi_2$ , are approximated as follows:

$$\Phi_1 = \Phi_m + \Delta\Phi_m \cos \frac{2\pi}{\tau}x + \Phi_i - \Delta\Phi_i \cos \frac{2\pi}{\tau}2x \quad [\text{Wb}], \quad (1)$$

$$\Phi_2 = -\Phi_m + \Delta\Phi_m \cos \frac{2\pi}{\tau}x + \Phi_i - \Delta\Phi_i \cos \frac{2\pi}{\tau}2x \quad [\text{Wb}], \quad (2)$$

where

$\Phi_i$ : the flux of the first harmonic by the exciting current,

$\Phi_m$ : the flux of the first harmonic by the permanent magnet,

$\Delta\Phi_i$ : the mean value of the flux by the exciting current,

$\Delta\Phi_m$ : the mean value of the flux by the permanent magnet.

In the one-phase excitation of CLPM, the thrust,  $F_1$ , is given by the gradient of the magnetic energy,  $W_m$ , to the displacement,  $x$ .

Therefore, the thrust,  $F_1$ , is given by<sup>3)</sup>

$$F_1 = \frac{dW_m}{dx} = \frac{d}{dx} \int NI d\Phi_1$$

$$= -\frac{2\pi NI}{\tau} \Delta\phi_m \sin \frac{2\pi}{\tau} x + \frac{2\pi NI}{\tau} \Delta\phi_i \sin \frac{2\pi}{\tau} 2x \quad [\text{N}], \quad (3)$$

where  $NI$  [A] is the magnetomotive force per coil.

In the two-phase excitation, the thrust,  $F_2$ , is given as follows:

$$F_2 = F_1(x + \tau/8) + F_1(x - \tau/8) = -\frac{2\sqrt{2}\pi NI}{\tau} \Delta\phi_m \sin \frac{2\pi}{\tau} x \quad [\text{N}]. \quad (4)$$

#### 4. Experimental results

##### 4.1 Static characteristics

The stator and mover are made of carbon steel material, S25C. The toroidal core of S25C for measurement of magnetic characteristics has an external diameter of 30 mm, an internal diameter of 20 mm, and a height of 10 mm. The primary and secondary windings are wound on the toroidal core, the number of turns for each being 200. The direct-current hysteresis loop of the annealed carbon steel, S25C, is shown in Fig.7. As is evident from Fig.7, the maximum flux density,  $B_m$ , at  $H=10$  kA/m is 1.75 T (Tesla), the residual flux density,  $B_r$ , is 1.2 T, and the coercive force,  $H_c$ , is 230 A/m.

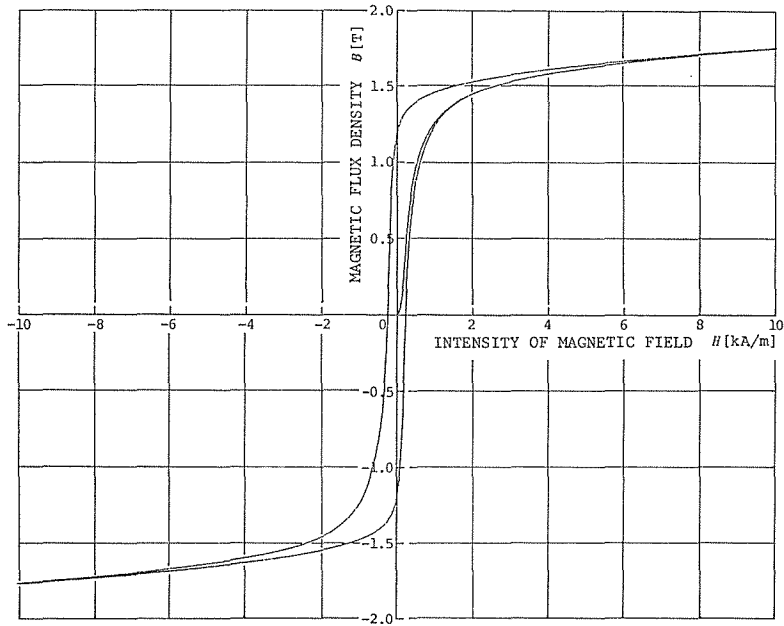


Fig.7 Direct-current hysteresis loop of the annealed carbon steel, S25C.

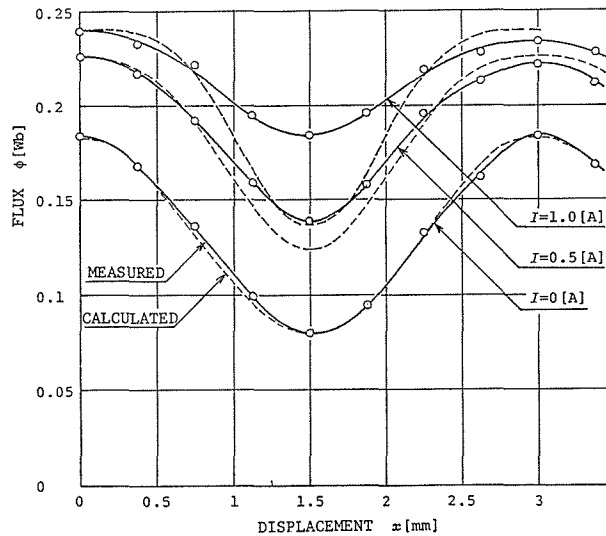


Fig.8 Flux distribution to the displacement of CLPM.

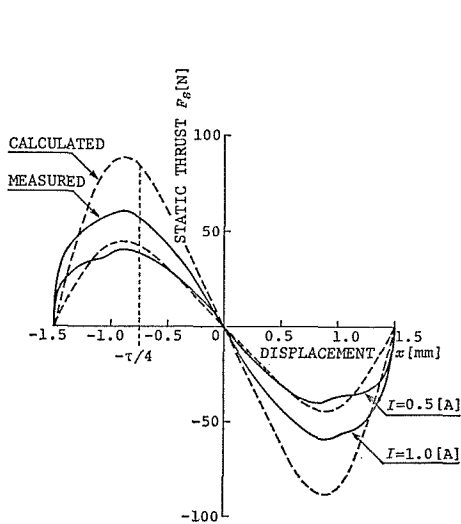


Fig.9 Static thrust versus displacement characteristics for one-phase excitation of CLPM.

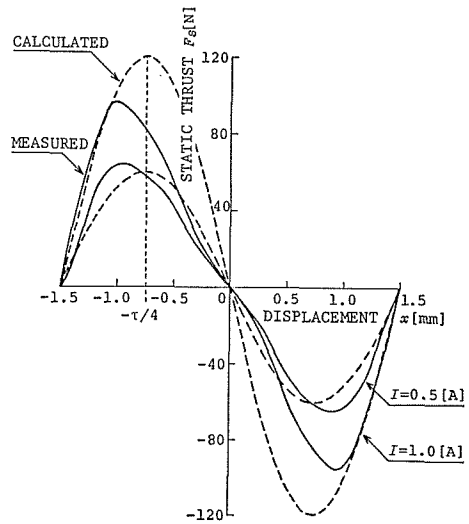


Fig.10 Static thrust versus displacement characteristics for two-phase excitation of CLPM.

The flux distribution with respect to the displacement of CLPM is shown in Fig.8. For the measurement of the flux, a search coil with 5 turns is wound around a tooth on the mover. The dotted lines represent the values calculated by Eqs. (1) and (2). As the exciting current is increased, differences are increased between the measured and calculated values because of magnetic saturation.

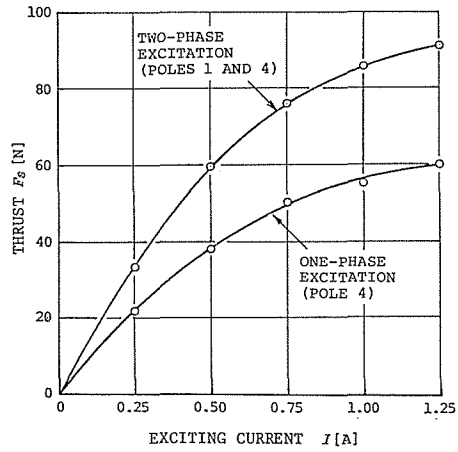


Fig. 11 Dependence of the static thrust of CLPM on the exciting current at the displacement  $x=\tau/4$ .

Table 1 Mechanical specifications of CLPM, Model CLPM-H16.

Item	Symbol	Value and unit
Stator		
Number of teeth	$n$	2 per pole
Pitch	$\tau$	3 mm
Width of tooth	$a$	1.5 mm
Width of slot	$q$	1.5 mm
Depth of slot	$d$	1.5 mm
Length of air gap	$\delta$	0.05 mm
Mover		
Pitch	$\tau$	3.0 mm
Width of tooth	$a$	1.5 mm
Width of slot	$q$	1.5 mm
Depth of slot	$d$	0.75 mm
Stroke	$L_s$	25 mm
Velocity	$v$	40 mm/s

Table 2 Electrical specifications of CLPM, Model CLPM-H16.

Item	Symbol	Value and unit
Number of poles	$m$	4
Number of turns of coil	$N$	390 turns
Exciting current	$I$	1.0 A
Impressed voltage	$V$	8.0 V
Coil resistance	$R$	8.0 $\Omega$ /coil
Magnetomotive force	$NI$	390 A/coil
Static thrust (two-phase excitation)	$F_s$	86 N
Maximum starting pulse rate	$f_s$	125 pulses/s

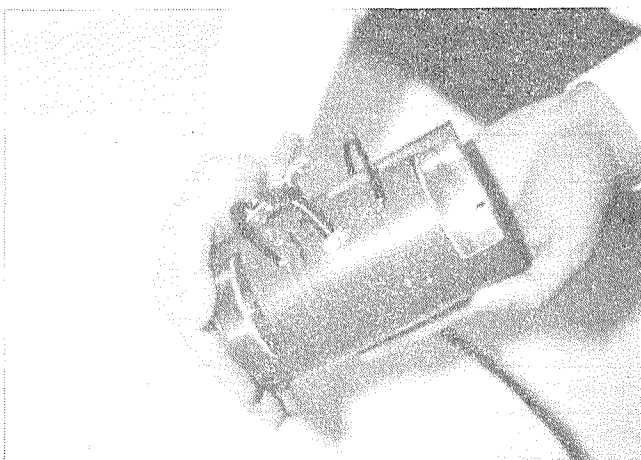


Fig. 12 A perspective view of the actuator for the artificial heart with CLPM, Model CLPM-H16.

Figure 9 shows the static thrust versus displacement characteristics for one-phase excitation of CLPM. In the measurement, the output of the linear potentiometer for displacement measurement was sent to the X-axis of an X-Y recorder. The mover was connected directly to the load cell, and jointed to the power cylinder by bolts. The output of the load cell was fed to the Y-axis of the X-Y recorder through a strain amplifier. The peak value of the static thrust for an exciting current of 1.0 A was obtained as 48 N (N : Newtons) at the displacement  $x=\tau/4$  (0.75 mm). Figure 10 shows the static thrust versus displacement characteristics for two-phase excitation of CLPM. The measured values are indicated by the solid lines, and calculated values by dotted lines. The peak value of the



static thrust for an exciting current of 1.0 A was obtained as 86 N by the experiment.

The dependence of the static thrust of CLPM on the exciting current at displacement  $x=\tau/4$  is shown in Fig.11. In the one-phase excitation, only the thrust by pole 4 is shown. In the two-phase excitation, the thrust by poles 1 and 4 is shown in Fig.11. These curves exhibit a saturation trend at exciting currents more than 0.5A.

The mechanical and electrical specifications of CLPM, Model CLPM-H16, are tabulated in Tables 1 and 2, respectively.

Figure 12 shows a perspective view of the actuator for the artificial heart. The mass of the entire actuator is 1.7 kg, the mass of the CLPM proper without the two rooms for sacs being 1.3 kg.

**4.2 Kinetic characteristics**

When the mass of mover is 0.25 kg, a maximum starting pulse rate of 125 pps (pulses per second) is obtained experimentally for two-phase excitation. Wave shapes of voltage,  $V$ , current,  $I$ , and displacement,  $x$ , are shown in Fig. 13. The velocity of 40 mm/s can be obtained in the stroke range from 12 to 25 mm for two-phase excitation.

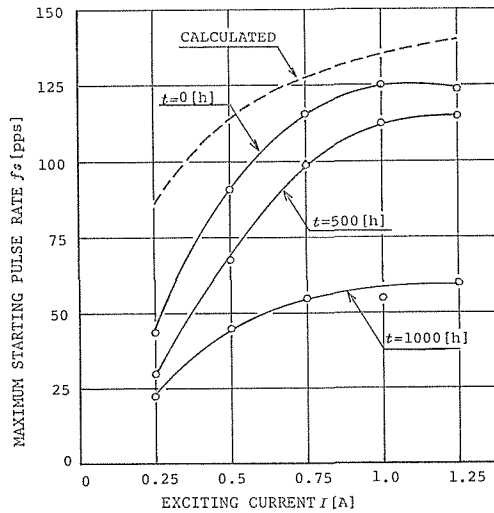
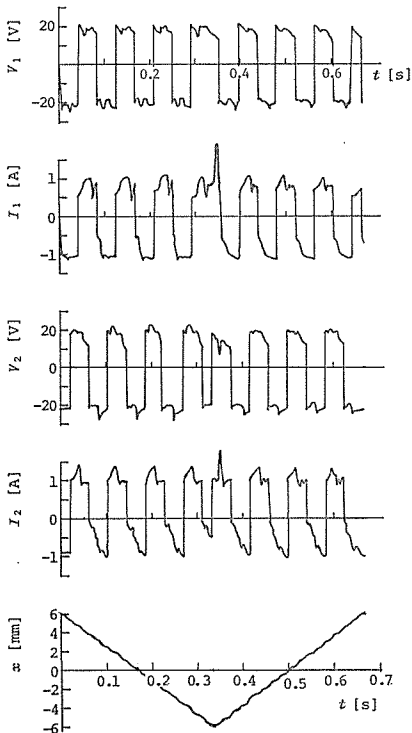


Fig. 14 Relation between the maximum starting pulse rate,  $f_s$ , and the exciting current,  $I$ .

Fig. 13 Wave shapes of voltage,  $V$ , current,  $I$ , and displacement,  $x$ , of Model CLPM-H16.

The maximum starting pulse rate,  $f_s$ , of a flat-type linear pulse motor is given by<sup>4)</sup>

$$f_s = 8\sqrt{\frac{K_f I}{2\pi m\tau}} \quad [\text{pps}], \quad (5)$$

where  $K_f$  [N/A] is the force constant and  $m$  is the mass of mover.

Figure 14 shows the relation between the maximum starting pulse rate,  $f_s$ , and the exciting current,  $I$ . The dotted line represents values calculated by Eq. (5). It was found that the difference between the calculated and measured values depends on the configurations of the linear pulse motors. Moreover, the value of  $f_s$  is also limited by the operating duration of CLPM. It could be confirmed by the experiment that the decrease in the pulse rate,  $f_s$ , with the operating duration  $t$ , is effected by both change in magnetomotive force of the permanent magnets and expansion in interval of the air gap with a rise in temperature of CLPM.

Figure 15 shows the temperature rise,  $\Delta T$ , of the surface of CLPM at room temperature. The experimental conditions were the ambient temperature 18°C and the pulse rate 40 pps in two-phase excitation with 1.0 A.

The temperature rise relative to the ambient temperature amounted to 39°C three hours after switching. The thermal time constant of CLPM is approximately 60 minutes as estimated from Fig. 15.

Figure. 16 shows the relation between the calculated flow rate and the heart rate for two-phase excitation. The flow rate,  $V_f$ , is calculated by

$$V_f = S L_s f_h \times 10^{-3} \quad [\text{L/min}], \quad (6)$$

where  $S$ : the cross-section of the pushing plate,  $(3.15)^2 \times \pi \text{ cm}^2$ ,

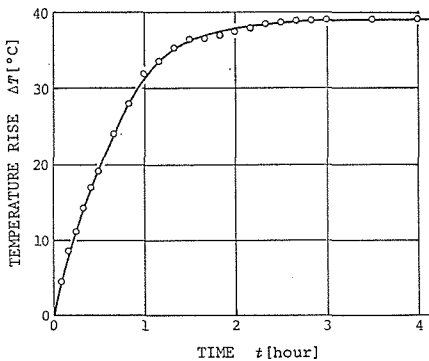


Fig. 15 Temperature rise,  $\Delta T$ , of the surface of CLPM at room temperature.

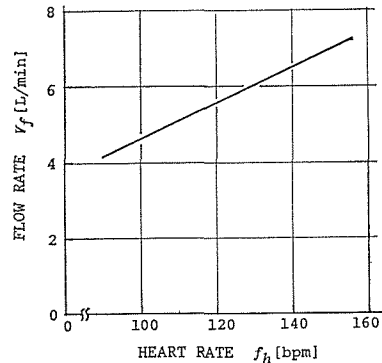


Fig. 16 Relation between the calculated flow rate and the heart rate for two-phase excitation.

$L_s$  : the stroke (= 1.5 cm).

$f_h$  : the heart rate in bpm (beats per minute).

The actuator has a driving capacity of 4 to 7 L/min (L : liter) in the range of heart rate from 90 to 156 bpm. A capacity more than 10 L/min is needed for a calf to live.<sup>5)</sup>

Figure 17 shows a perspective view of the unit of the actuator for the artificial heart using the CLPM, Model AHA-H16. A scale of 30 cm and a box of cigarette

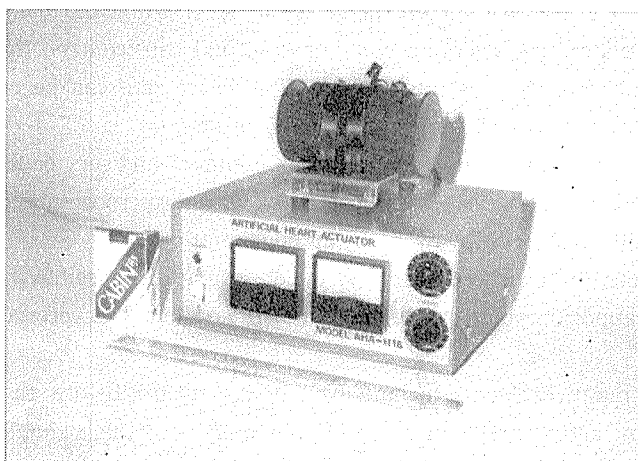


Fig.17 A perspective view of the unit of actuator for the artificial heart using CLPM, Model AHA-H16.

Table 3 Characteristic values of CLPM-H16

Item	Symbol	Value and unit	Remarks
Static thrust	$F_s$	86 N	Two-phase excitation
Input power	$P_i$	16 W	1A × 8V × 2
Volume	$V$	0.27 L	Real volume of CLPM
Mass	$M$	1.28 kg	Real mass of CLPM
Ratio of thrust to input power	$F_s/P_i$	5375 N/kW	
Ratio of thrust to volume	$F_s/V$	317 N/L	
Ratio of thrust to mass	$F_s/M$	67 N/kg	
Force constant	$K_f$	136 N/A	
Ratio of thrust to acting area	$F_s/A$	15.2 N/cm <sup>2</sup>	A is tota area of acting tooth.
Ratio of thrust to electromotive force	$F_s/A \cdot NI$	0.02 N/cm <sup>2</sup> ·A	NI is electromotive force.

are placed near the unit in Fig. 17. The total mass of the actuator, AHA-H16, with the source and driver included, is only 5.4 kg.

Main characteristic values of CLPM-H16 are tabulated in Table 3. These characteristic values are superior to those of ordinary linear pulse motors.<sup>6)</sup>

## 5. Conclusion

The following points have been disclosed by the present investigation on the actuator for the artificial heart, Model AHA-H16:

1) The actuator is completely noiseless in its driving and has good manipulation. The actuator has a simple configuration and can control the thrust of 60 to 85 N by changing the exciting current. The heart rate can be controlled from 90 to 156 bpm for stroke 25 mm with high accuracy.

2) The actuator has many merits in maintenance and service lifetime because of fewer component elements. When combined with a microcomputer, the actuator operates the full stroke with lower power consumption.

3) The actuator has been made portable; it may be possible that its size will be reduced to approximately one tenth that of the ordinary air-pressure generating unit.

There are many problems to be solved in the future before the actuator can be applied to an actual artificial heart. For example, methods should be found out to suppress the temperature rise and to shield the leakage flux around the CLPM.

It will be possible for an advanced actuator using a linear motor to generate a flow rate more than 10-20 L/min in the range 50-200 bpm.

Acknowledgement: The authors would like to thank ex-Professor, K. Taguchi, M.D., Ph.D., Hiroshima University for suggesting this work and stimulating their interest in it. The authors wish to express their gratitudes to Mr. H. Wakiwaka, Technical Manager, Ono Sokki Co. Ltd., Dr. K. Yamakawa, Chief Engineer, Hitachi Metals Co. Ltd., and Mr. S. Yamamoto, Senior Researcher, Amada Co. Ltd. for frequent stimulations and helpful discussions. The authors wish also to thank Professor, Dr. I. Matsuzaki, Department of Synthetic Chemistry, Shinshu University, for reading and correcting the manuscript for this paper.

A part of this research was supported by a Scientific Fund from the Ministry of Education of Japan.

**REFERENCES**

- 1) The Asahi Shimbun of 25 March, 1983 (in Japanese).
- 2) H. Yamada, T. Mizuno, K. Taguchi, S. Fukunaga, N. Nishizawa, Y. Ibaragi, and Y. Hara: Development of Artificial Heart Actuator Using Linear Pulse Motor, IEEJ, Tech. Meet. Magnetics, MAG-82-81, 1-17, 1983 (in Japanese).
- 3) H. Yamada, T. Mizuno, T. Shinkai, H. Shimada, Y. Yamamoto, S. Kamioka, and K. Ozaki: Thrust Characteristics of Cylindrical Linear Pulse Motor, IEEJ, Tech. Meet. Magnetics, MAG-83-11, 19-28, 1983 (in Japanese).
- 4) Y. Yamamoto, H. Yamada, and T. Mizuno: Starting Pulse Rate of a Flat Type Linear Pulse Motor, IEEJ, Vol. 103, No. 5-B, 374, 1983 (in Japanese).
- 5) H. Yamada, K. Taguchi, S. Fukunaga, S. Tagami, and N. Nishizawa: Development of Actuator for Artificial Heart Using Linear Pulse Motor, 4th Congress of the International Society for Artificial Organs, 7 (a), 14, 1983.
- 6) The Magnetic Actuator Technical Committee: Linear Motors and Their Applications (Book), Inst. Elect. Eng. Japan, 203-205, 1984 (in Japanese).